Journal of
Computational and Theoretical Nanoscience
Vol. 16, 1–6, 2019

Preparation and Development of Ceramic System Catio$_3$ for Used Medical Applications

Fadhil K. Farhan[1,*], Mohammed O. Kadhim[2], and Shahlaa J. Ashour[3]

[1]*AL-Karkh University of Science, College of Science, Department of Medical Physics*
[2]*AL-Karkh University of Science, College of Remote Sensing and Geophysics, Department of Remote Sensing*
[3]*Ministry of Science & Technology*

In this study, $CaTiO_3$ powder was prepared by mixing the extracted and prepared calcium oxide from egg shells and nanotube dioxide in an effective mechanical mixing method. XRD and XRF were used to determine the crystalline structure and compounds involved in the preparation of the material at temperatures of 1150 °C. SEM and SPM techniques were used to diagnose the crystalline shape and particle size of the prepared material. The results of the XRD test showed the phase formation of $CaTiO_3$ at angles 2Θ (33.787, 27.5047, 47.5907) at a mean size of 32 nm granularity calculated using the Scherer equation. The results of the XRF test showed the matching of the reaction material and the appearance of clear peaks for TiO_2 and CaO. SEM images showed homogeneous distribution and clear granular form formed at temperature 1150 °C. The SPM results were also cleared to calculate the granular distribution rate of the prepared material at 44 nm. The models were modeled in SBF solution for 30 days to determine whether they were suitable for human body or not. The results showed that a layer of solution was present on the surface of the model and showed efficacy against the bacteria through the halo formed around the sample. Physical tests such as hardness, compressive strength, thermal diffusion and density were also performed.

Keywords: $CaTiO_3$, Active Mechanical Blend, XRF, SEM, SBF.

RESEARCH ARTICLE

1. INTRODUCTION

Nanotechnology, otherwise called atomic nanotechnology alternately sub-atomic engineering, includes that union Also characterization from claiming practical biomaterials with nanoscale Characteristics What's more molecule sizes more modest over 100 nm. Nanostructure biomaterials need aid a improvement What's more cam wood offer mechanical, electric, magnetic, chemical, optical and living offers predominant over customary biomaterials with micrometric microstructures. Bioactive pottery has got to be a standout amongst those major fields over drug. In the most recent three decades.[2] One amazing triumph of bioactive pottery will be the clinical utilizationf sintered hydroxyapatite (HA) for implants because of its bioactivity and conductivity.[7,8] Electro pottery have various requisitions because of their particular structures What's more physical properties, for example, interconnect, bundling also substrates materials for microelectronics or Likewise singular out components, especially as capacitors alternately sensors. Calcium titanate ($CaTiO_3$) will be a ceramic material for a perovskite structure. This compound doesn't demonstrate anisotropy, and its structure is cubic over 1307 °C, tetragonal the middle of 1107 Furthermore 1227 °C What's more orthorhombic underneath 1107 °C.[14] The cubic perovskite structure might make got during room temperature at doped for cation receptors. $CaTiO_3$ indicates unique structural, electrical also optical properties and, therefore, may be from claiming extraordinary experimental and innovative premium.[6] Titanium oxide (TiO_2) have distinctive requisitions in the food, cosmetics, aero spatial. Moreover biomedical domains Since it holds a bioinert phase. Additionally might aggravate osteo-integratable of the touching tissue.[7] TiO_2 secured close by nanoparticle structure might extend advantageous levels to bioactivity, pushing bone tissue burgeoning ahead nanoparticles and main pick osseointegration, osteoinduction. In addition tissue association with biomaterial interfaces.[10] For repairing bone harm initiated by trauma, surgical resection What's more intrinsic disfigurement corrections, bone tissue building will be of service.[11,12] As new biomaterials, bioinorganic and the use of metal ions in the synthesis of new materials have received substantial attention.[15] Bioactive materials

*Author to whom correspondence should be addressed.

are qualified by their close connection with living bone via hydroxyapatite formation.[17] The results indicated that a very important group of materials is based on CaO-TiO_2 and CaO-Al_2O_3-TiO_2 systems that might be used as novel bioactive materials for bone regeneration.[13] Past investigations have demonstrated that framework ($CaAlTiO_6$) pottery needed a greater amount mechanical quality and bioactivity over Ca-P pottery.[11] Bone may be a composite regular living tissue which comprises of a natural stage in which calcium holding inorganic stage crystals would insert.[3,4] Bone by weight holds something like 30% matrix, 60% mineral and 10% water A. Those bone grid is essential collagen which answerable for those rigidity (Alhanassiou et al., 2000). Mineral part from bone is calcium phosphate, which imparts compressive quality of the bone tissue.[4] Studied amalgamation and characterization about bioactive forsterite nano-powder established Forsterite. Also provskite ceramic may be another bioceramic with useful biocompatibility. Studied union what's more characterization from claiming HA/*n*-TiO_2 Nanocomposites for bone tissue recovery, those HA (hydroxyapatite) utilized. Similarly as bone grid in this fill in might have been prepared toward those biomaterials.[9] Studied Tribological conduct technique for bone against $CaTiO_3$ covering to recreated body liquid (SBF). In spite of $CaTiO_3$ need been recommended as a covering to biomedical applications, a characterization of tribological properties simulating human states need not been reported.[5]

2. EXPERIMENTAL AND MATERIALS USED

The starting materials for the preparation of calcium titanate, $CaTiO_3$ were $CaCO_3$ and TiO_2 (rutile type) of purity $>99 \cdot 99\%$, grain size 44 nm. A reactive form of CaO, obtained from eggshells after clinking and crushing to semi-powders and then burned in reaction furnace at 450 °C, 700 °C, 900 °C was obtained on powder $CaCO_3$ and was decomposition in electrical furnace at 1100 °C. The calcium Oxide was handled carefully to prevent the adsorption of CO_2 and H_2O from ambient air. The rutile form of TiO_2 was dried at 500 °C before use. Calcium titanate $CaTiO_3$ were prepared by active mechanical mixtures method of 1:CaO and 1:TiO_2 in the appropriate molar ratio 1:1 for milling 12 h. Prepared material from blending process was reaction at temperature 1250 °C. Completion of the reaction was confirmed by powder X-ray diffraction (XRD) and (XRF) analysis of the product. The calcium titanates powder had the orthorhombic structure with cell parameters $a = 5.441\ A^0$, $b = 7.642\ A^0$, and $c = 5.440\ A^0$; and had provskite system. The powder mixtures of component oxides were pelletized at 200 MPa using a steel die with 20 mm diameter for sintering at 1325 °C. The product powder was investigated and appointed by (XRF) analysis and SEM test. The powder density was measurement by tow method; Arkamides and dimensions at various temperatures (1150 °C–1325 °C). Mechanical properties of

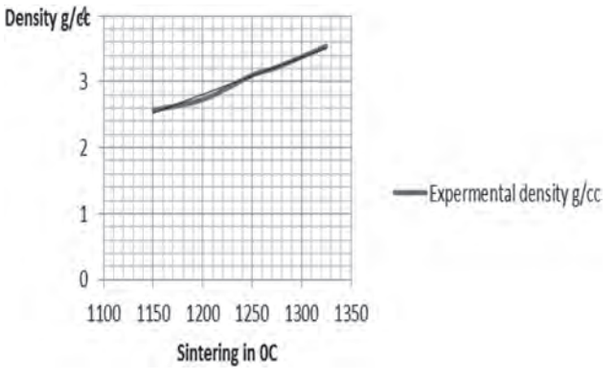

Fig. 1. Experimental density at various sintering.

prepared samples were test by micro-hardiness and compression strength. The thermal conductivity measurement of disk sample ($d = 20$ mm) by TCi devices.

3. RESULTS AND DISCUSSION

3.1. Density Measurement

Ex Experimental density was measured by Arkamides and dimensions method where results showed increases and enhancement of density at temperature increases show Figure 1 this due to best mixture and completion reaction between CaO and TiO_2 powders the best of density at sintering 1325 °C (3.54 g/cc) compared with theoretical density (3.75 g/cc). When this sintering interaction became particles of material more adhesion and more shrinkage causing an increases in density.

3.2. XRD-Test

Figure 2 shows the XRD pattern of the sample after different thermal cycles. The dominant XRD peaks belong to perovskite calcium titanate ($CaTiO_3$) phase. However, peaks of minor intensity corresponding to the precursor phases TiO_2 and CaO are still observed even after cycles of thermal treatment. It seems that the sample with molar ratio Ca/Ti = 1 has smaller amount of undesirable secondary phases (CaO and TiO_2). Figure 2 shows the XRD diffract grams of the Nano-composite powders obtained by heat treatment at 1200 °C/2 h, indicating a decrease in peak intensity in the CaO phase, an increase in peak intensity in the $CaTiO_3$ phase, of the orthorhombic crystal

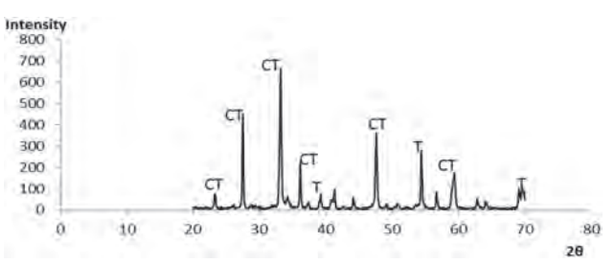

Fig. 2. XRD pattern of sample $CaTiO_3$.

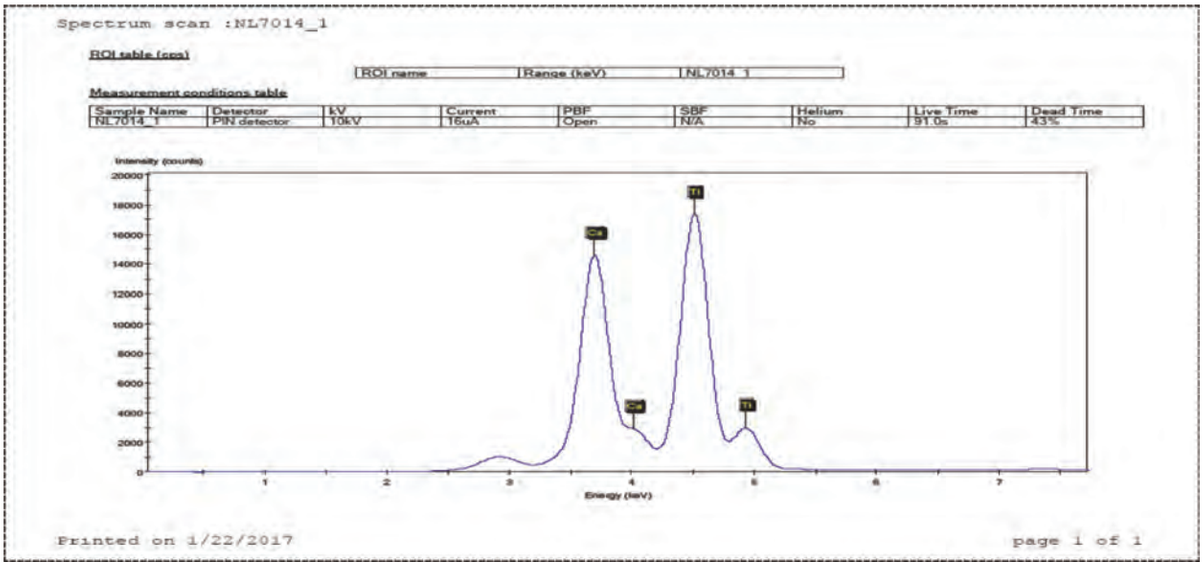

Fig. 3. XRF-analysis of $CaTiO_3$ concretions.

(a)

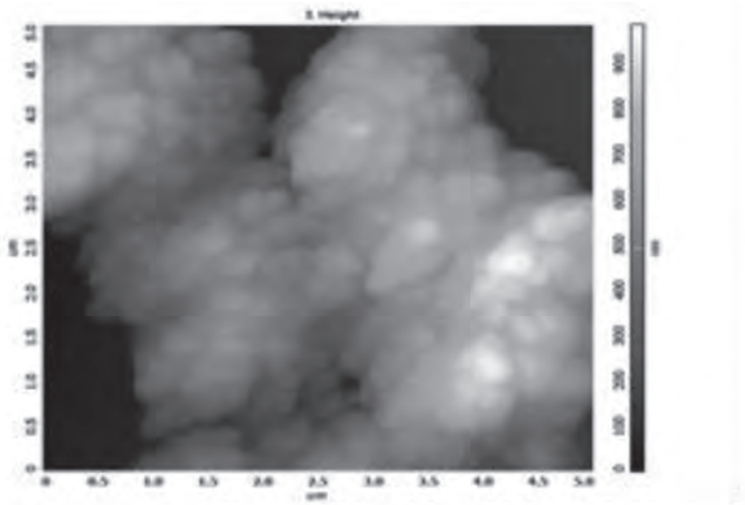

(b)

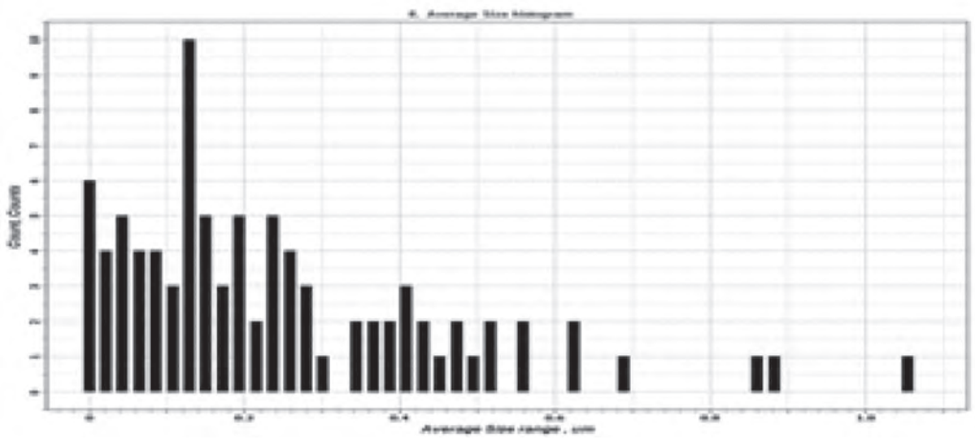

Fig. 4. SPM-test: (a) Grain size 2D image, (b) grain size distribution.

RESEARCH ARTICLE

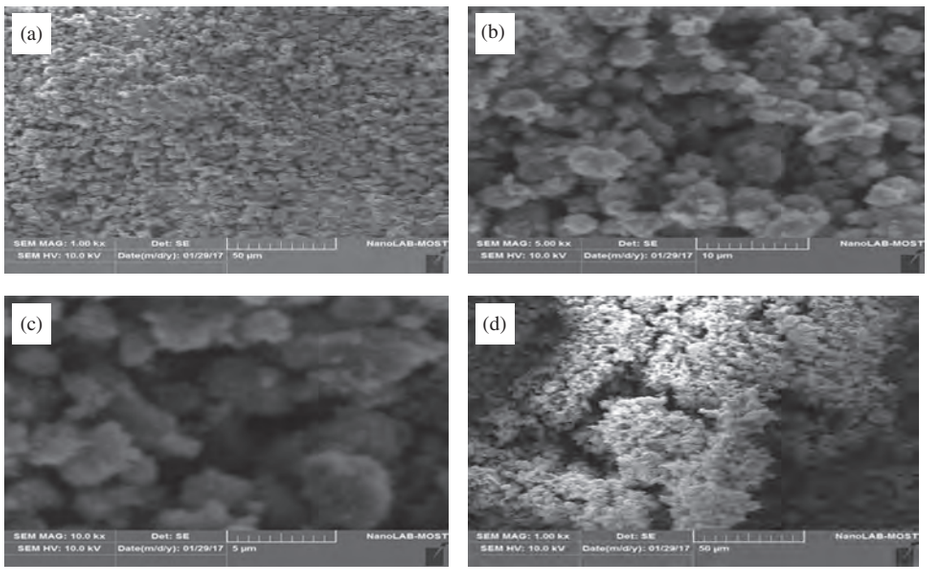

Fig. 5. Morphology SEM patterns of $CaTiO_3$: (a) Sintering 1150 °C, (b) sintering 1200 °C, (c) sintering 1250 °C and (d) sintering 1325 °C.

system and the presence of low intensity peaks in the TiO_2 phase. This may have caused a change in the interfacial diffusion kinetics, favoring the dissociation of Ca^{++} ions to form $CaTiO_3$ phase (CT). The presence of $CaTiO_3$ phase in the orthorhombic structure of biomaterial compositions has been described in the literature. The grain size average of papered powder it is (38 nm) measurement by Scherrer equation.

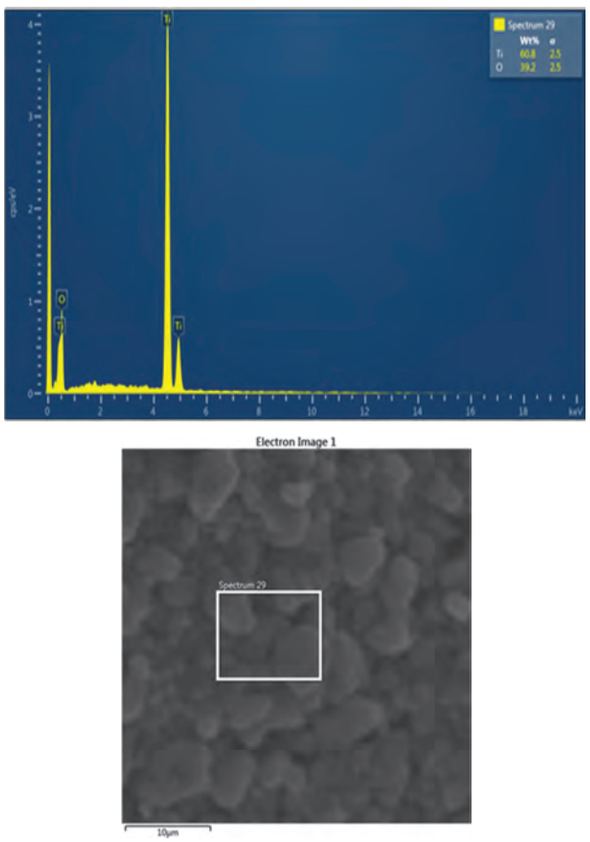

Fig. 6. Morphology SEM and EDS spectrum pattern of n-TiO_2.

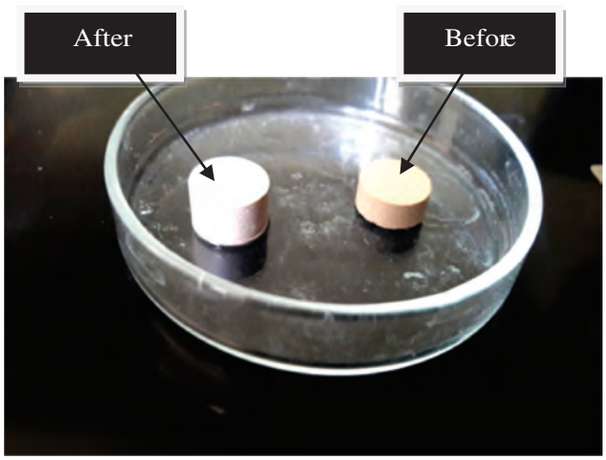

Fig. 7. Photographic image of samples before and after immersion for 30 days.

3.3. XRF-Test

Figure 3 shows the XRF pattern of the sample after sintering and pressing. The dominant XRF peaks belong to Calcium Oxide CaO, dioxide titanium TiO_2, so the high and low of intensity this back to percentage of content

Table I. SBF solution concentration g/l.

NaCl	KCl	$MgSo_4 \cdot 7H_2O$	$CaCl_2H_2O$	Na_2HPo_4	KH_2Po_4	$NaHCO_3$
8.0	0.4	0.2	0.185	0.0166	0.06	0.35

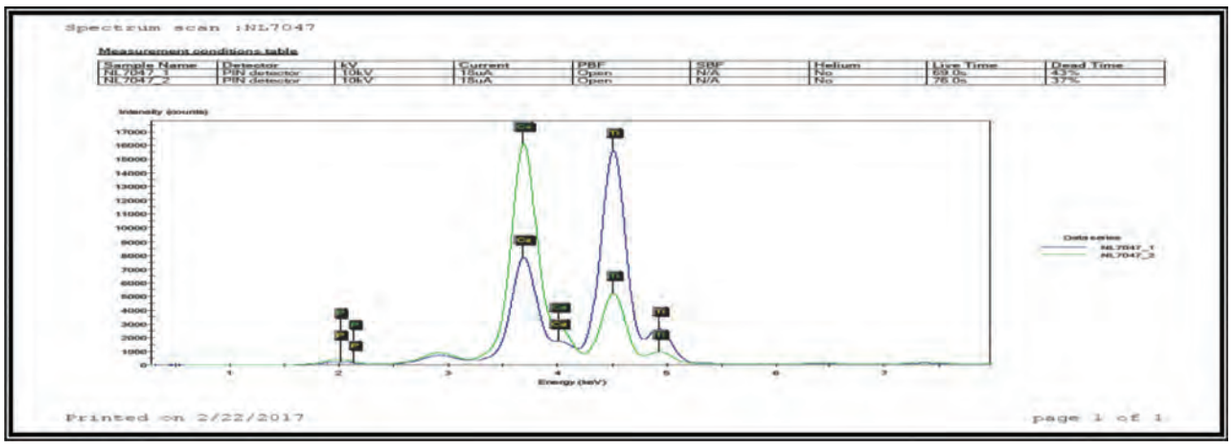

Fig. 8. XRF-analysis after simulated body fluid (SBF) immersion.

powders. From figure showed results match between experimental and test. This may have caused the accuracy of mixing and pure materials used.

3.4. SPM-Test

The SPM distribution of grain size and image of Nanosystem $CaTiO_3$ is shown in Figure 4, the measurement result showed the distribution of grain size average (43 nm) with 2D image. Through this test we confirmed that prepared system by mechanical active mixture method gave uniform distribution and the same or closed to the value particle size average that got from XRD-by Scherrer's equation.

3.5. SEM-Test

The Morphology SEM patterns of $CaTiO_3$ are shown in Figure 5. This seemed to composite of domains formed by a large number of closely packed clusters appears to be uniform. Figures 5(a)–(d) shown a SEM micrograph of Nano-structured milled TiO_2 powder, whose morphology is characterized by agglomerated particles with sizes smaller than (100 m), therefore the granular composite heat treated at 1150 °C/2 hrs, 1200 °C/2 hrs, 1250 °C/2 hrs and 1325 °C/2 h respectively, showed granules with deferent sections and interconnected granular micro porosity was also observed. The micrographs of Nano-system depicted in figures clearly show secondary phase (n-TiO_2) well dispersed in the CaO matrix this is agreement with Ref. [1]. Figure 5(d) showed Morphology the prepared system at sintering 1325 °C more closely packed clusters and pores structure. Figure 6 shown the Morphology SEM and EDS spectrum pattern of n-TiO_2.

3.6. Simulated Body Fluid TEST

The baulk sample with dia. (10 mm) used to Simulated body fluid SBF Test. Figure 7 shows photographic image of samples before and after immersion for 30 days. The image shown formation of hydroxapatiate (HA) layer

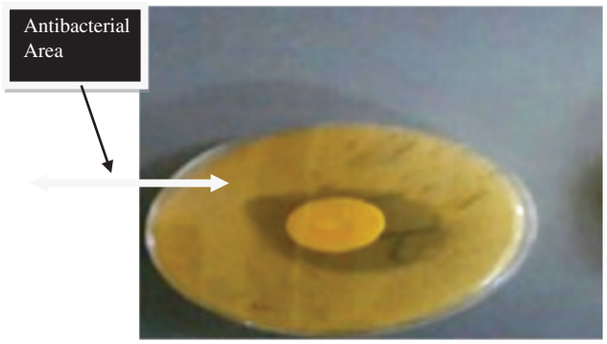

Fig. 9. Photographic image of sample during antibacterial test.

adhesion on the sample surface. The chemical composition of SBF solution concentration g/l in Table I. Figure 8 Shown XRF-analysis of $CaTiO_3$ and $(PO_4)_2$ after immersion.

3.7. Antibacterial Test

Figure 9 shows the antibacterial effect of prepared ceramic system as well as the examination of toxic and it is clear from the image the surrounding area around the sample present antibacterial resistance and can be calculated by diameter of rate surrounding area is 40 mm.

4. CONCLUSION

Nanosystem calcium titanate biomaterials need aid present research topics, which demonstrate guaranteeing biomedical utilization in orthopedic, trauma treatment, What's more dental provisions. This new era for biomaterials displays new morphologic aspects. As far as granules, grains and microspores, giving ideal states for bone neo-structuring. Also reproduction about bone tissue. The Nanosystem powders high temperature treated. In 1300 °C/2 h demonstrated a decrease in the crest of the CaO and TiO_2 period. Also an expand in that of the power peaks ct phase, coming about because of

RESEARCH ARTICLE

expanding temperatures throughout those heat medicine. Those micrographs from claiming processed powders demonstrated agglomerate nanoparticle morphologies. The optional nanometric TiO_2 stage likewise discovered will be well scattered in the calcium oxide grid. In this contemplate it might have been closed that the material readied in this best approach demonstrated. An secondary viability against the microscopic organisms and in addition those helter skelter bond of the calcium phosphate layer in the result comparative of the body liquid framed on the surface of the material, making it more suitableness for medicinal applications, particularly for bone payment.

References

1. K. A. Athanasiou, C. D. Zhu, R. Lanctot, C. M. Agrawal, and X. Wang, *Tissue Eng.* 6, 361 **(2000)**.
2. C. Carter and M. Norton, Ceramic Materials: Science and Engineering, Springer, New York **(2007)**.
3. F. C. Driessens, *Z. Naturfor. Sect. C* 35, 357 **(1980)**.
4. F. C. Driessens, J. W. Dijk, and J. M. Borggreven, *Calcif. Tissue Res.* 26, 127 **(1978)**.
5. M. A. Encinas-Romero, S. Aguayo-Salinas, J. L. Valenzuela-García, S. R. Payán, and F. F. Castillón-Barraza, *Int. J. Appl. Ceram. Technol.* 7, 164 **(2010)**.
6. C. J. Kennedy and B. C. Howard Chakoumakos, *J. Phys.-Condens. Mater.* 6, 1479 **(1999)**.
7. G. Kolodiazhnyi, M. Annino, T. Spreader, R. Taniguchi, F. Freer, and A. Azough, *Act Mate.* 57, 3402 **(2009)**.
8. A. Kurella and N. B. Dahotre, *J. Biomaterial. Appl.* 20, 5 **(2005)**.
9. M. Kharaziha and H. Fathi, *Synthesis and Characterization of Bioactive Forsterite Nanopowder Ceram, In. J.* 35, 2449 **(2009)**.
10. J. Khang and T. J. Haberstroh, *Biomat.* 29, 970 **(2008)**.
11. Q. Liu, L. Cen, S. Yin, L. Chen, G. Liu, and J. Chang, *Biomat.* 29, 4792 **(2008)**.
12. G. Liu, C. Wu, W. Fan, X. Miao, D. C. Sin, and R. Crawford, *J. Biomed. Mater. Res. B Appl. Biomater.* 96, 360 **(2011)**.
13. P. Byuvol, L. Gabsalikhova, I. Makarova, E. Mukhametdinov, and G. Sadygova, *Astra Salvensis* 373 **(2017)**.
14. A. J. Moulson and J. M. Herbert, Electroceramics: Materials, Properties, Applications, 2nd edn., John Wiley, New York **(2003)**.
15. H. Mohammadi, M. Hafezi, N. Nezafati, S. Heasarki, A. Nadernezhad, and S. Ghazanfari, *J. Ceram. Sci. Technol.* 5, 1 **(2014)**.
16. H. A. Nelson, S. Camargo, and G. Enori, *Am. J. Biometal. Eng.* 2, 41 **(2012)**.
17. A. Srivastava and R. Pyare, *Int., J. Sci. Technol. Res.* 1, 28 **(2012)**.

Received: 1 February 2018. Accepted: 11 March 2018.

RESEARCH ARTICLE